# Measurements of Plasma Energy Density and Conductivity from 3 to 120 Kilobars*

James W. Robinson†

Department of Electrical Engineering

The University of Michigan

Ann Arbor, Michigan

ABSTRACT

Plasma energy density, conductivity, and temperature were measured at various pressures ranging from 3 to 120 kilobars. The experimental work was conducted in two parts; plasmas with pressures to 15 kilobars were formed by capacitor discharges in water, and plasmas with higher pressures were formed by detonating 10 grams of PETN in the water adjacent to the electrical discharge path. At 9.4 kilobars and 35 000$^{o}$K, the energy density was 15 J/mm$^{3}$. An equation of state based upon the Debye shielding theory, without accounting for the distortion of electron quantum states, predicts an energy density of only 3.3 J/mm$^{3}$. An approximate calculation is presented which accounts for these distortions, and furnishes an estimate of particle densities from measured energy densities. A peak energy density of 75 J/mm$^{3}$ was obtained at 117 kilobars and $10^{29}$ atoms/m$^{3}$. At 10 kilobars and 35 000$^{o}$K, the conductivity was 3 x $10^{5}$ (ohm m)$^{-1}$ and increased with pressure. At 110 kilobars and 10 000$^{o}$K, the conductivity was 2.5 x $10^{5}$ (ohm m)$^{-1}$ and also was an increasing function of pressure.

# I. INTRODUCTION

Plasma energy density and conductivity have been measured at pressures ranging from 3 to 120 kilobars. Various theoretical studies of high density plasmas have appeared which are generalizations upon the Debye shielding theory.[1-3] However, data were not then available to check results. The present measurements show that the Debye theory and its modifications are not accurate. The distortion of electron quantum states dominates the shielding effect at high density.

The present results are the outgrowth of experimental procedures previously reported by E. A. Martin,[4] who made some measurements in the lower portion of the pressure range being considered here. His plasmas were formed by discharging a capacitor bank between electrodes submerged in water; the pressure was produced by the inertial restraint of the water upon the expanding discharge column. Higher pressures than Martin's were obtained in the present work by detonating a chemical explosive in the water near the discharge path.[5] Experimental modifications have improved the accuracy of measurements and increased the time resolution above the levels he attained. Changes in the computational procedures have eliminated approximations which caused his pressure estimates to be too high.

The experimental procedures and calculations are described in section II. The data and results of calculations are then presented for measurements near 10 kilobars in section III and for measurements near 100 kilobars in section IV. Section V concludes the paper with a discussion of theory pertaining mainly to the measurements at the lower pressures, where calculations based upon the Debye shielding theory predict values for internal energy five times smaller than measured values.

## II. EXPERIMENTAL PROCEDURES

Although experimental findings are presented for two different regions of pressure, the procedures for obtaining data were not substantially different in the two cases. The necessary changes in procedure arose from the use of a chemical explosive to confine the plasma at the higher pressure level.

### Formation of Plasma

For both regions of pressure, a bank of energy storage capacitors formed the plasma between under-water electrodes spaced a few millimeters apart. The bank, designed to keep inductance low, was rated at 20 kV and contained up to 56μF. Rates of current rise less than maximum were obtained by either removing capacitance or increasing the circuit inductance. For all tests,

the charging voltage was kept at 20 kV to minimize variations in the formative time of the discharge. The rate of current rise was nearly constant while data were being recorded except for the first 0.2 μsec. when the rate was somewhat less.

A fine wire was stretched between the electrodes to establish the discharge path and to eliminate a time jitter of about 1 μsec in the formation of the discharge. The jitter could not be tolerated when explosive was used because the shock wave from the explosive had to be synchronized with the electrical discharge. The plasma consisted mainly of water vapor, with only a small fraction of the mass in the plasma being from the wire. Because of the low mobility of ions in the plasma,[4] the metal from the wire remained concentrated on the axis of the discharge column, and also the metal from the electrodes did not migrate any significant distance into the plasma. Wires of 0.001 in. tungsten and 0.000[illegible] in. copper were used successfully, with no apparent difference in the results. However, jitter occurred with wire of 0.0005 in. tungsten.

## Measurements

Photographs were taken of the discharge columns with a Kerr-cell camera designed to take two exposures during a single experiment. A beam-splitting mirror behind the lens formed two light channels which were shuttered independently. Exposure times were 0.1 μsec.

The magnification factor of the camera was measured so that plasma dimensions could be scaled from the photographs.

The density of the photographic image indicated the temperature of the plasma. The plasma radiated as a blackbody, so the intensity of radiation upon the film could be computed as a function of temperature. The measurements had only a slight dependence upon the spectral characteristics of the film and camera. The plasma temperature was determined for one set of experimental conditions with a photodiode using Martin's procedure.[4] Then photographs were taken of that source of known temperature to calibrate the film density scale against the camera f number and the plasma temperature. ~~Thus two measurements of temperature were obtained for each experiment, and variations of temperature from one part of a plasma column to another could be measured.~~ The application of the Debye theory is not highly sensitive to temperature so that the conclusions are unaffected by this somewhat imprecise method of temperature measurement.

The discharge circuit was attached to the ground plane at one of the discharge electrodes and at that point only. Then the voltage of the other electrode relative to ground was the same as the drop across the plasma. This voltage was measured with a 1000X probe and oscilloscope. However, a correction was necessary to account for the inductance of the electrodes and the plasma itself. The correction was measured by replacing

the plasma with a heavy copper wire, and by computing the difference in inductance between the wire and plasma as a second order correction. The correction to the voltage drop across the plasma column, given by d(LI)/dt, was from 10 to 20%.

## Calculations

Plasma volume was computed as a function of time from the diameter and length of the discharge column. The diameter was found to be nearly proportional to time during the first microsecond of column growth in all of the experiments. A slight blurring occurred in the photographs because of the plasma growth during the exposure. Thus the time of a particular photograph was chosen to be the end point of the 0.1 μsec exposure interval, and the diameter to include the outermost fringes of the photographic image.

Pressure in the plasma was produced in two ways. The water surrounding the plasma provided an inertial confinement, and the pinch effect provided a magnetic confinement. The total pressure was taken to be the sum of the two contributions.

The discussion of the inertial effect, considered first, is sufficiently general to include tests with or without explosive. An expanding cylinder of plasma displaces water which has a certain ambient pressure, 1 bar for the tests without explosive, and 100 kilobars

for the tests with explosive. The plasma pressure exceeds the ambient pressure by an amount related to the expansion rate.

For the computation of pressure in the plasma, the initial assumptions, subject to later revision, are that the pressure is uniform throughout the plasma and that there is no mass transfer across the boundary of the plasma. Also, because of experimental fact, the growth rate is assumed to be constant. The radially expanding plasma column is surrounded by a cylindrically symmetric region of water compressed above the ambient pressure, and separated from the ambient region by a concentric shock front. The pressure distribution and the mass velocity distribution are computed for this region.

The method used for the calculation was that of Taylor as described by Courant and Friedrichs.[6] However the differential equations of conservation were written in cylindrical instead of spherical symmetry. The equation of state for water was

$$p + B = (p_o + B)\ (\rho/\rho_o)^{\gamma} \qquad (1)$$

where p is pressure, $\rho$ is density, $\gamma = 7$, $B = 3140 \times 10^5$ N/m$^2$, and the subscript represents 1 atmosphere and 20°C. The mathematical assumption was made that the dependent variables were functions only of the ratio of plasma

column radius to time r/t and not upon r or t individually. Then the problem was reduced to solving

$$\frac{dC}{dU} = \left(\frac{C}{U}\right) \frac{(1-U)^2 - C^2 - (\gamma-1)U(1-U)/2}{(1-U)^2 - 2C^2} \qquad (2)$$

where C and U are sound and mass velocity normalized by the ratio of r/t. This equation is analogous to (162.04) of Courant and Friedrichs. After (2) is solved, the unknowns can all be found by quadratures. The calculations were performed by a digital computer for different values of ambient pressure, and the results are plotted in Fig. 1, where the pressure at the surface of the expanding cylinder is shown as a function of the expansion rate. Intuitively, one expects the pressure to approach the ambient pressure as the growth rate is reduced. The dashed line of Fig. 1 illustrates this for 100 kilobars of ambient pressure. However, for small growth rates, a departure is observed from the anticipated trend. Apparently, r/t cannot be treated as the independent variable for such conditions.

The displacement rate of the water is not as great as the plasma expansion indicates, because water is inducted into the plasma at its boundary. The effective rate is then the actual rate times the factor

$$f = 1 - (n/n_o)^{1/2} \qquad (3)$$

where n is the atomic density of the plasma, and $n_o$ of the water at ambient pressure. This factor is found by noting that a cylinder of water of unit diameter expands to form a plasma column of diameter $(n_o/n)^{1/2}$. The effective expansion is then $(n_o/n)^{1/2} - 1$ instead of $(n_o/n)^{1/2}$. The factor f becomes increasingly important as plasma density increases. The effect of uneven pressure in the plasma would mean a higher average pressure than boundary pressure; this effect is neglected as it has little importance in the results to follow.

The plasma is constricted by the interaction of its current with its self-magnetic field. If R is the radius of the column, then the pressure as a function of the radius r is given by

$$p(r) = \int_r^R J(r)\, B(r)\, dr \qquad (4)$$

where J is current density and B is magnetic flux density. Pressure is zero on the boundary and increases toward the center depending upon the current distribution in the discharge. The average pinch pressure $p_{av}$ is given by

$$p_{av} = \mu I^2/(8\pi^2 R^2)$$

regardless of the radial current distribution, and (5) was used in the calculations. For the special case of a uniform current distribution, the peak pressure on the axis is twice the average.

Power is the product of current and corrected

voltage, and the integral of power is the energy delivered to the plasma. The energy losses because of mechanical work on the surrounding water and because of radiation are subtracted from the total energy; the result is divided by the plasma volume to obtain the average energy density of the plasma.

The conductivity of the plasma column is computed from the current, the corrected voltage, and the dimensions of the column.

## Use of Explosives

The use of explosives requires an integrated design for the electrodes and explosive charge. The detonation in the explosive must be synchronized with the electrical discharge, and the pressure generated by the explosive must be measured.

The electrode design is shown in Fig. 2. The entire assembly was immersed in water for an experiment, so that the space between the electrodes was filled with water. When the explosive was detonated, a region of high pressure was established in the water between the explosive-water interface and the upward-moving shock front. The plasma was formed at the location of the initiating wire in the region of high pressure after the shock front had passed.

A sensor wire was buried in the explosive to detect the passage of the detonation front. The detonation

gases shorted the wire to the steel casing around the explosive, and a voltage pulse was thereby generated. This reference pulse was transmitted through delay circuits and amplified to actuate the various instruments and to initiate the capacitor discharge with a three-electrode spark gap switch.

The pressure behind the shock front was computed from measurements of the velocity of the front.[7] For the explosive PETN which was used, the shock velocity was approximately 5 mm/μsec and the corresponding pressure was 100 kilobars. Thus 100 kilobars was the ambient pressure used in applying the results of Fig. 1. For the cases of interest here, the effective growth rate considering correction (3) was about 200 m/sec and the effect of column expansion was completely negligible. A correction to the ambient pressure arises from the gradient of the pressure behind the shock front. Since the plasma is not located exactly at the shock front, but some distance behind it, the pressure is somewhat different from that at the shock front. The gradient was computed, following Harris,[8] from the deceleration of the shock front and from the estimated curvature of the front. The figure of 100 kilobars was on the order of 10 to 15% high. However, for the results to follow, this correction was neglected as it was the same for all experiments. The variation in pressure from shot to shot must have been small; otherwise the observed data trends would have been obscured.

## III. RESULTS FROM 3 TO 15 KILOBARS

When no explosive was used, the rate of current rise was adjusted over a 10 to 1 range to produce different pressures in the plasma. Of course, the electrode design could be considerably simpler than that of Fig. 2. For any given experiment, the pressure did not vary significantly with time up to a microsecond, but remained at a steady value determined by the rate of rise. Likewise the other intensive properties of the plasma remained practically constant even though the discharge column was expanding radially.

The data from late in the observation interval are most accurate because the radius and current are relatively large and easily measured. For a series of identical tests, the measured data were reproducible within $\pm$ 10%. Each data point in the graphs of this section was determined from an average over three identical tests.

The energy losses from the plasma were on the order of 5% or less, and they were neglected. The corrections (3) to the column expansion rates for computing pressure were determined from estimates of density in the theoretical discussion.

The radius of the discharge column at 1 μsec is shown in Fig. 3 as a function of the current at 1 μsec. In Fig. 4, the pressure from inertial effects and the

total pressure averaged over the volume are shown as a function of current, again with values at 1 μsec. The difference between the two curves of Fig. 4 is the average pinch pressure, which is seen to increase with increasing current. At approximately $10^{11}$ A/sec, the inertial and pinch effects contribute equally to pressure.

The internal energy density is shown in Fig. 5 as a function of the total average pressure, and the two quantities are approximately proportional. The conductivity is shown in Fig. 6, again as a function of the total pressure. Conductivity increases with pressure, and as a consequence the current would tend to concentrate on the axis of the discharge column where pressure is greatest.

The measurements of temperature showed no trends related to the other data. For all of the experiments, the measured temperature was 35 000°K, with a scatter of approximately ± 20% in the points.

## IV. RESULTS FROM 100 to 120 KILOBARS

As the rate of current rise was varied in the experiments with explosive, the pressure varied according to the pinch effect which was superimposed upon the ambient pressure of 100 kilobars.

The data shown here are for a point in time 0.3 μsec after the initiating of the electrical discharge. The

individual experiments instead of averages. For the larger values of the rate of current rise, a rapidly increasing pinch effect caused abrupt changes in the data trends, which would be somewhat obscured by an averaging process.

For the experiments with explosive, the energy lost by mechanical work was more significant than for experiments without explosive, so a correction was included in the calculations.

The radius is shown in Fig. 7 as a function of current at 0.8 μsec after initiation of the electrical discharge. As the rate of current rise is increased, a critical value is reached where the growth rate of the plasma column is slowed by the pinch effect. But the data point for the highest value of current indicates that above the critical point, the pinch effect does not develop as strongly. Fig. 8 shows the pinch pressure developing with an increasing rate of current rise, yet the last point is much lower than the others preceding it.

The energy density varies with pressure as shown in Fig. 9. In this graph the data point corresponding to the maximum rate of current rise is indicated with a flag. It does not correspond to the highest energy density even though it represents the largest current of

any of the tests. A peak energy density of 75 $J/mm^3$ is achieved at the maximum pressure.

The conductivity is shown as a function of pressure in Fig. 10. The conductivity generally increases with pressure, the odd data point being the exception.

Temperatures for tests with explosives were much lower than for the other tests. The average was about 10 000°K, yet rather large fluctuations occurred even from one part of the plasma column to another. Whereas without explosive, the photographs showed a very uniform plasma, the high pressure plasmas often had uneven temperature patterns as shown in Fig. 11. Variations from 10 000°K were on the order of $\pm$ 20%.

## V. THEORETICAL CALCULATION OF ENERGY DENSITY

At a pressure of 10 kilobars and a temperature of 35 000°K, the energy density was measured to be 15 $J/mm^3$. Since temperature $\theta$ and pressure p together uniquely specify the properties of the plasma for a system in equilibrium,[4] the energy density u can be computed if an appropriate theoretical description of the plasma can be found.

One method of calculating u might be found in the Debye shielding theory which has been described by various authors.[9,10] Yet this approach was found to be inadequate.

From this theory, the potential energy of an ion in the field of the shielding cloud of charge is given by

$$c = -e^2/4\pi\epsilon_o h \qquad (6)$$

in mks units where h is the Debye length. When the theory is applied to a hydrogen-like plasma with electrons, ions, and neutrals, the quantity $c$ appears in Saha's equation and in equations expressing p and u. In Saha's equation, $c$ is a correction to the ionization potential and for the conditions of interest, it exceeds the ionization potential. A modification by Rouse eliminates this difficulty so that calculations may be performed. Then u is found to be 3.3 $J/mm^3$ with n being $1.6 \times 10^{27}$ $m^{-3}$ and with the ionization being 25% complete. Yet u was measured to be 15. The disagreement between theory and experiment illustrated in this case persisted for all of the data recorded without explosive. The Debye radius is smaller than the average interparticle spacing, so the inapplicability of the theory is not surprising. The Debye theory was even less appropriate for data taken with explosives where pressure was higher and temperature lower.

Harris[9] suggests that a theory must properly consider the effects of distortion of the bound electron quantum states because of the high particle density. The quantum states cannot be defined over a lattice as in a metal because of the randomness of the ion locations.

ions which fluctuate rapidly because of the high ion velocities in the plasma. The electrons do not contribute to pressure through translational motion,[9] and no distinction can be made between bound and free electrons.

One approach for considering the distortion of electron states is the use of the virial theorem as applied to a collection of particles with coulombic interactions. For a system of n ions and n electrons in a unit volume, let V be the expectation value of the potential energy and let T be the expectation value of the kinetic energy operator

$$-\Sigma_j(\hbar^2/2m_j)\nabla_j^2 \qquad (7)$$

summed over all particles. Then the virial theorem is

$$2t = -v + 3p/n \qquad (8)$$

where v is defined as V/n, and t as T/n.

If f represents the energy per particle pair for the imaginary process of converting liquid water into a collection of singly-ionized atoms and electrons with infinite spacing, then u is given by

$$u = n(f+v+t) \qquad (9)$$

where f is $26.9 \times 10^{-19}$J.

Assume that t is given by

$$t = t' + 3/2k\theta \qquad (10)$$

where $3/2k\theta$ is the contribution of the ion and t' is the contribution of the electron. Furthermore assume v to be the expectation value of the potential energy of

an electron in the field of the ion cluster. Like-particle interactions are neglected. Then by defining g as $-t'/v$ and c as $t' + v$, (8) and (9) can be written as

$$p = n\left[k\theta + c(1-2g)/3(1-g)\right] \tag{11}$$

and

$$u = n(f + c + 3/2k\theta) \tag{12}$$

For isolated atoms, g is 1/2 and (11) and (12) reduce to ideal gas equations. However, for high densities where the quantum states are distorted, g is different from 1/2 and a correction is introduced into the pressure equation. The formal calculation of c and g requires an average over the Fermi distribution of electrons in the various distorted quantum states. For a simple calculation, let c be given approximately as a function of $\theta$ by an average over the first two unperturbed states of the hydrogen atom. Then by using experimental data, values for n and g can be computed. Table 1 shows the results of such calculations. For a theoretical estimate of g in terms of n, the distorted ion potential function can be represented by the function $Kr^s$ where the virial theorem requires that $g = -1/2\ s$. The calculation is illustrated in Fig. 12 where $a_o$ is the Bohr radius and $r_o$ is given by $(3n/4\pi)^{1/3}$. For the values of n in Table 1, the corresponding theoretical values of g are 0.338, 0.324, and 0.316. Considering that values of g in the table are quite sensitive to

temperature, the agreement is very good.

The distortion of electron quantum states identified with a change in g results in a cohesive force through a correction to the kinetic pressure as seen in (11). The Debye theory also predicts a cohesive force which, however, is much lower in magnitude. Because of the distortion of quantum levels, the energy density and the particle density are much higher than the Debye theory predicts.

The plasmas at 100 kilobars have pressures 10 times greater and temperatures 3 times less than the plasmas at 10 kilobars. Therefore the particle densities are much higher. However the upper limit on particle density is the density of the water surrounding the column of plasma, which, with explosive, is $1.6 \times 10^{29} m^{-3}$. Since densities of $10^{28}$ are reached at 10 kilobars, then a reasonable estimate for the plasma density at 100 kilobars is $10^{29} m^{-3}$.

ACKNOWLEDGMENTS

H. C. Early offered many helpful suggestions in the experimental work. F. J. Martin, D. Engstrom, R. Petit, and J. Caister assisted with the experimental activities and the numerical computations. W. N. Lawrence constructed the Kerr-cell camera.

Table I. Values of n and g computed from experimental data. $\theta = 3.5 \times 10^4$ °K and $c = -18.7 \times 10^{-19}$ J.

| p (kilobars) | u ($J/mm^3$) | n ($m^{-3}$) | g (dimensionless) |
|---|---|---|---|
| 4.67 | 8.18 | $0.530 \times 10^{28}$ | 0.269 |
| 9.44 | 15.2 | 0.985 | 0.275 |
| 15.25 | 20.7 | 1.34 | 0.290 |

*This work was supported by a grant from the National Aeronautics and Space Administration.

†Present address: Electrical Engineering Department, Pennsylvania State University, University Park, Pennsylvania.

[1]H. S. Green, Nuclear Fusion (International) 1, 69-77, 1961.

[2]D. S. Villars, Phys. Fluids 6, 745-748, 1963.

[3]O. Theimer and R. Gentry, Ann. Phys. (N.Y.) 17, 93-113, 1962.

[4]E. A. Martin, J. Appl. Phys. 31, 255-267, 1960.

[5]J. W. Robinson, Appl. Phys. Letters 8, 207-208, 1966.

[6]R. Courant and K. O. Friedrichs, Supersonic Flow and Shock Waves (Interscience Publishers, Inc., New York, 1948), Chapter VI, pp. 424-28.

[7]J. M. Walsh and M. H. Rice, J. Chem. Phys. 26, 828, 1957.

[8]A. J. Harris, Underwater Explosion Research (Office of Naval Research, Department of the Navy, 1950), Vol. 1, pp. 1053-1056.

[9]G. M. Harris, Phys. Rev. 133A, 427-37, 1964.

[10]C. A. Rouse, Astrophys. J. 136, 636-664, 1962.

[11]C. A. Rouse, Astrophys. J. 136, 665, 1962.

LIST OF FIGURES

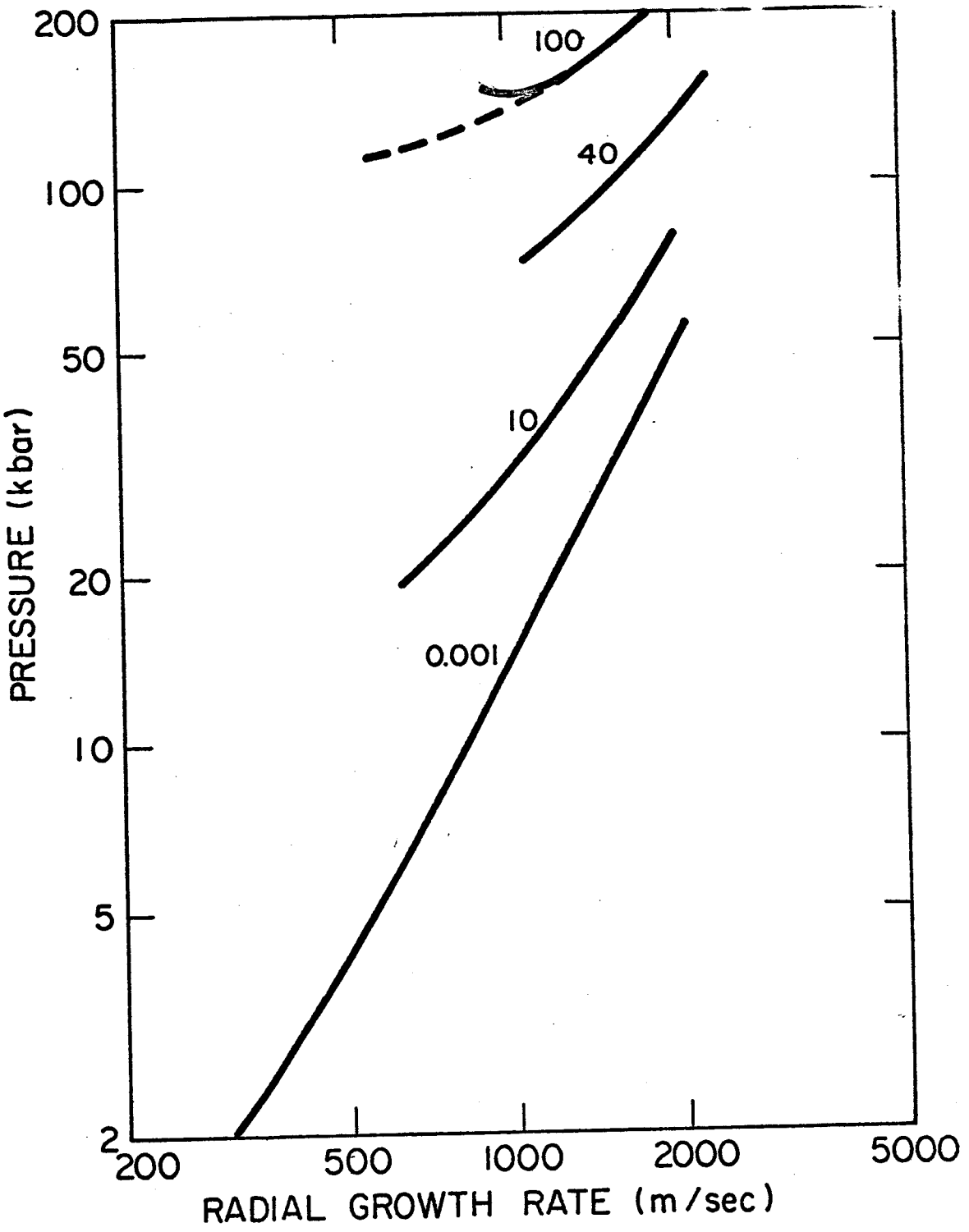
200
100
50
20
10
5
2
PRESSURE (k bar)
100
40
10
0.001
200
500
1000
2000
5000
RADIAL GROWTH RATE (m/sec)

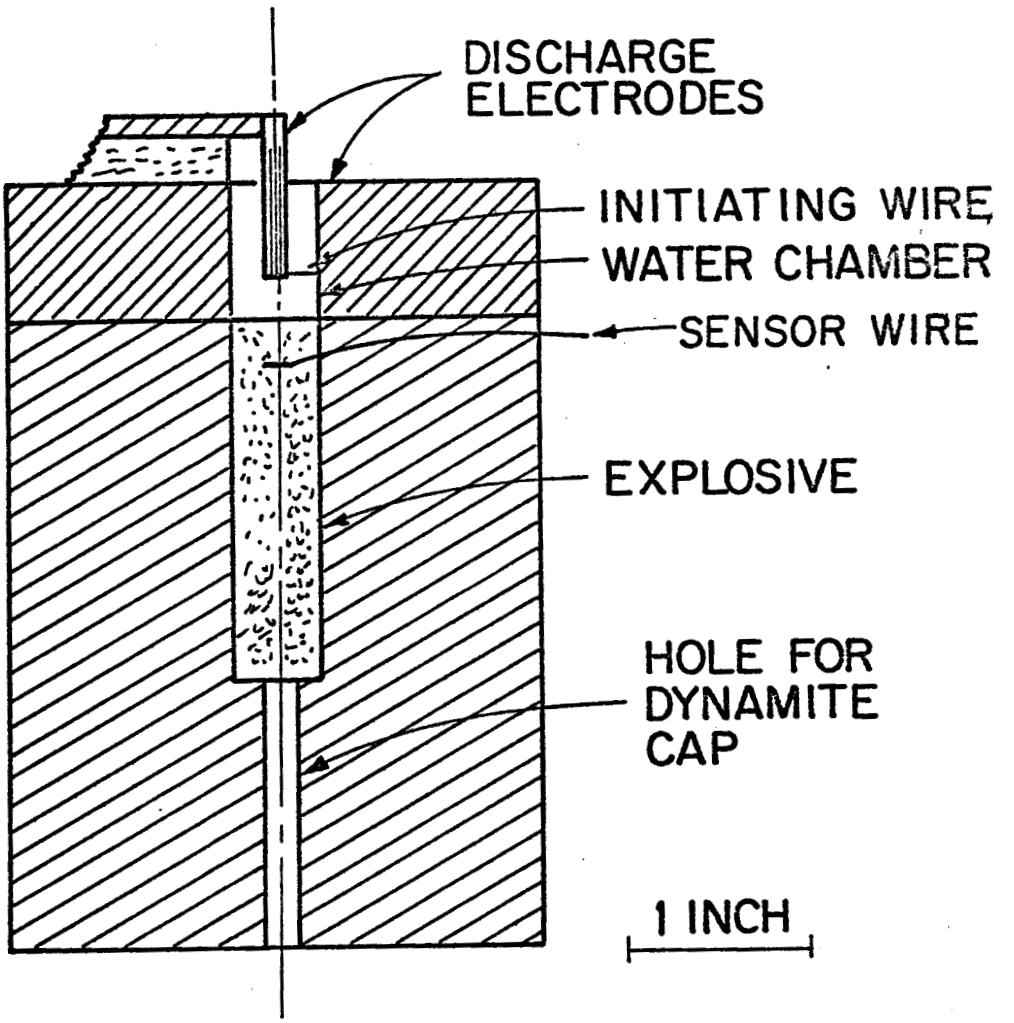


Fig. 2 James W. Robinson

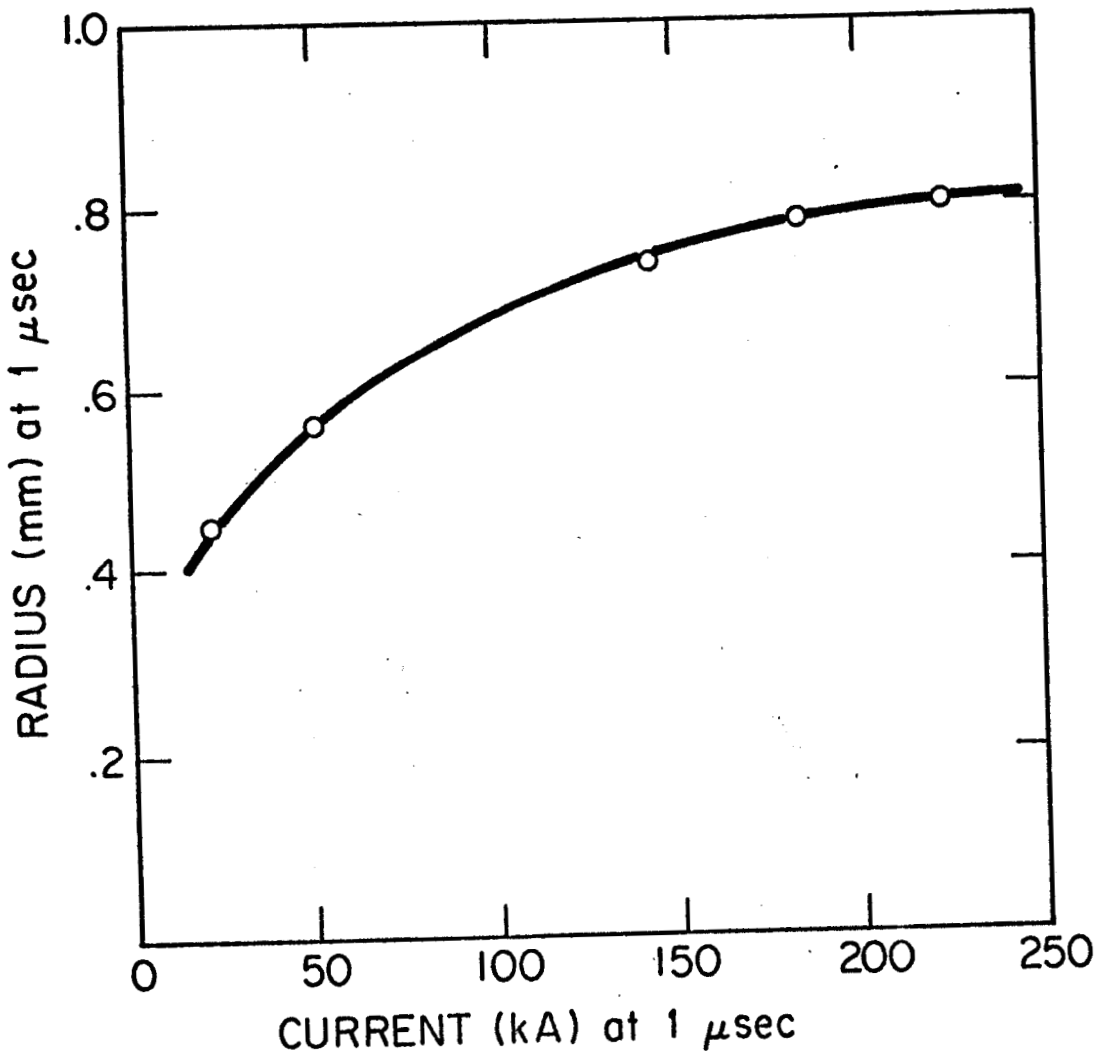


Fig. 3 Jet Velocity vs Radius at 1 μsec Plus

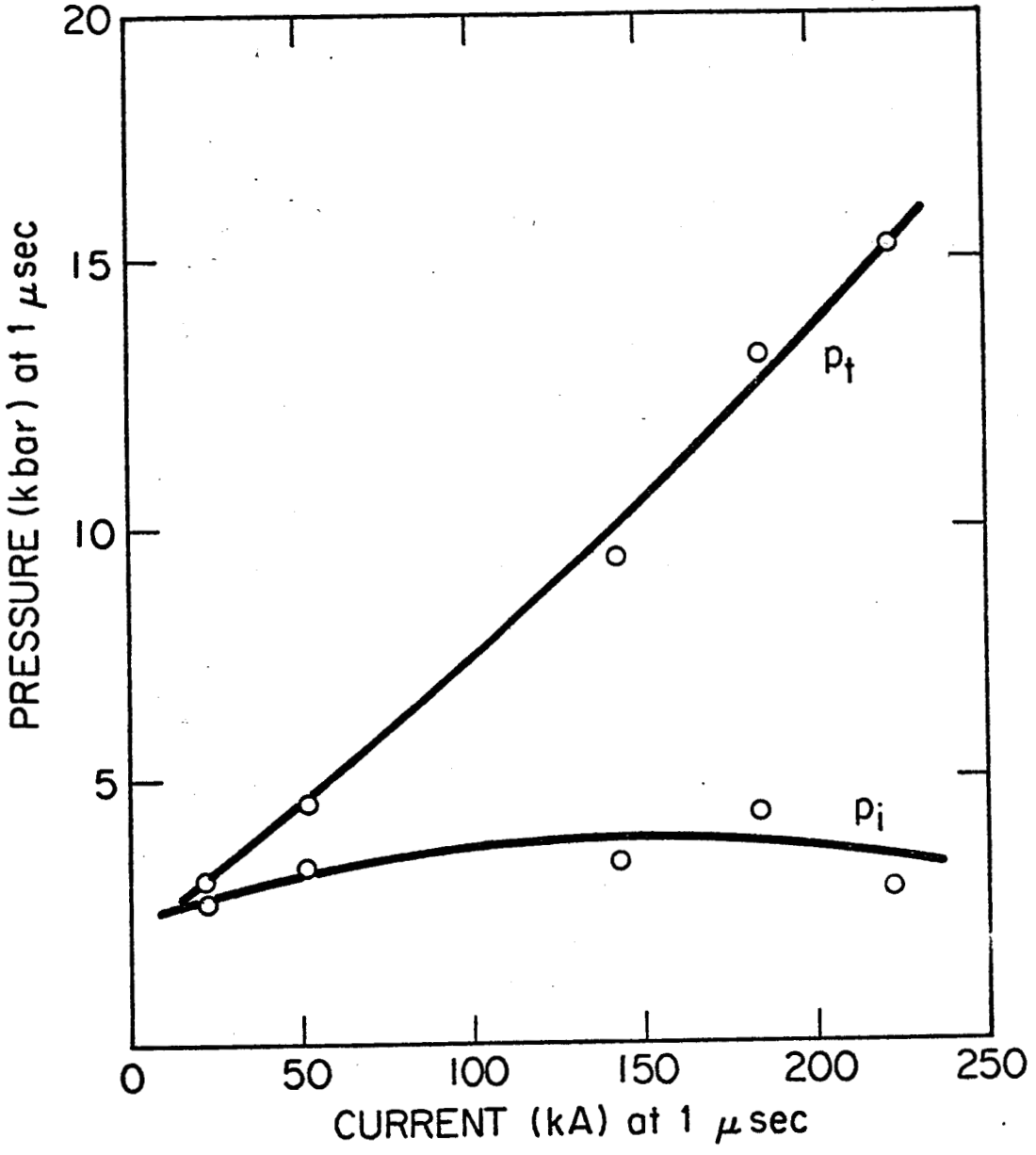


Fig. 4 James W. Robinson

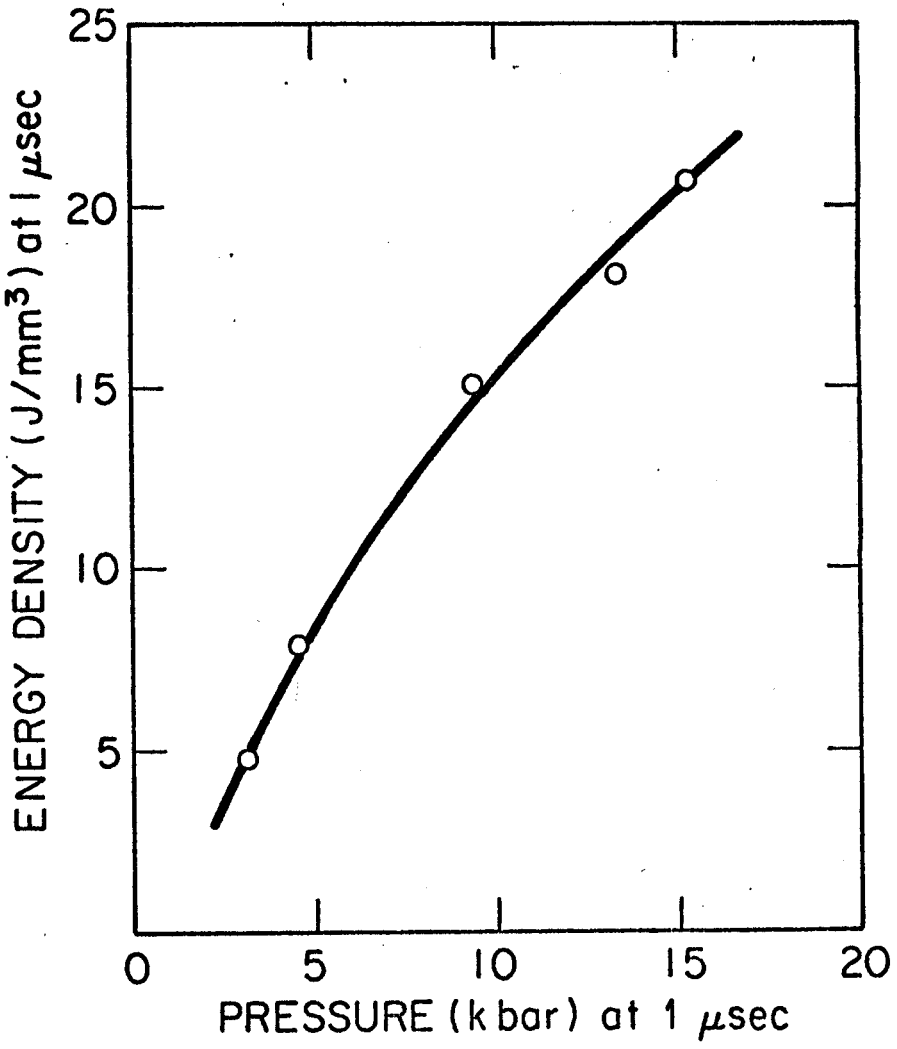


Fig. 5 James W Robinson J. Appl. Phys.

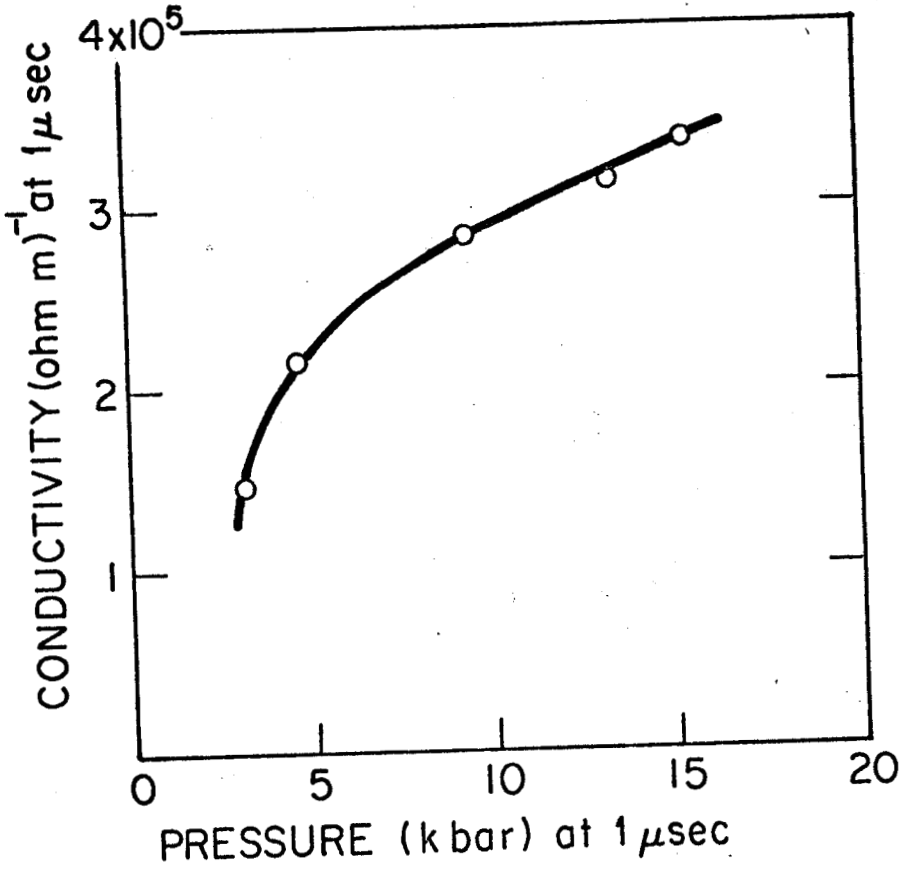


Fig. 6 James H. Robinson J. Appl. Phys.

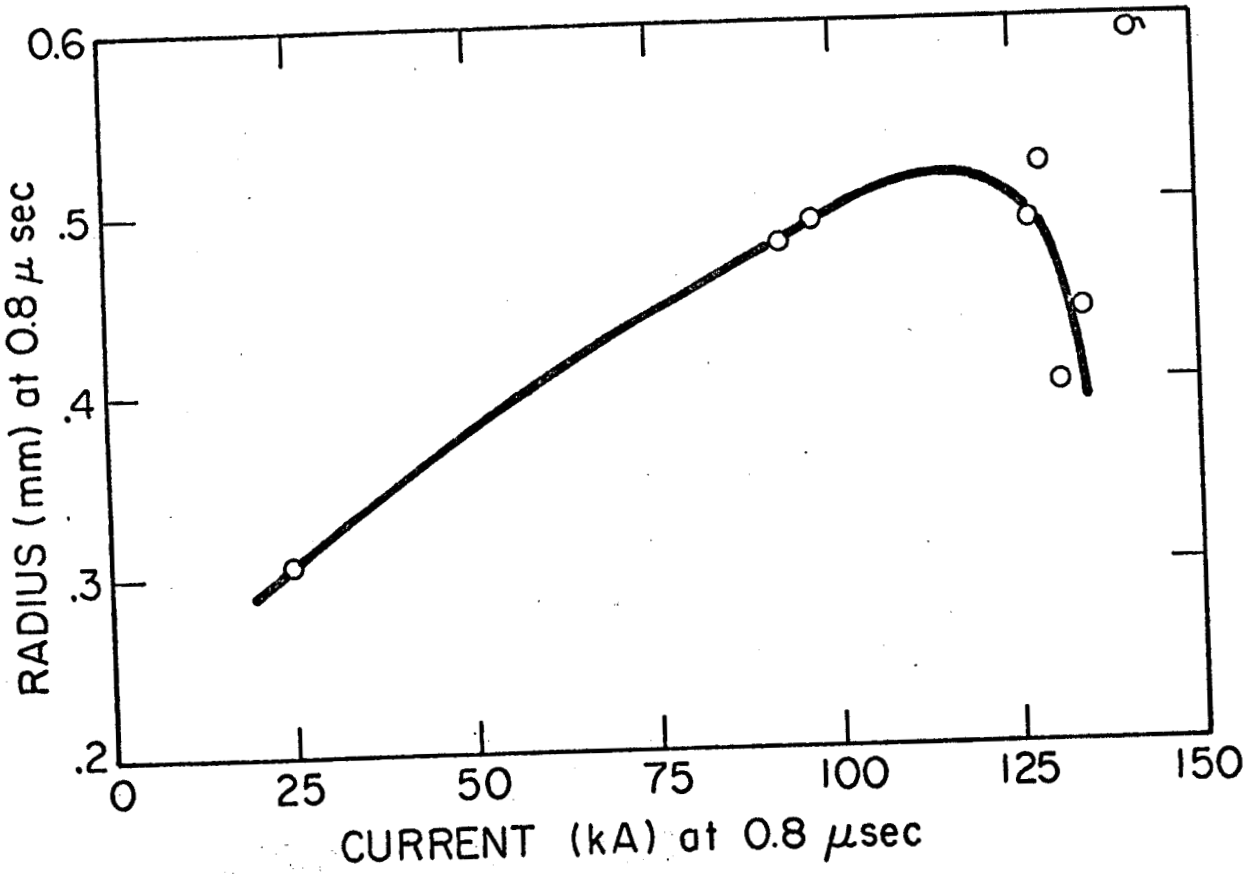


Fig. 7. James W Robinson J. Appl. Phys.

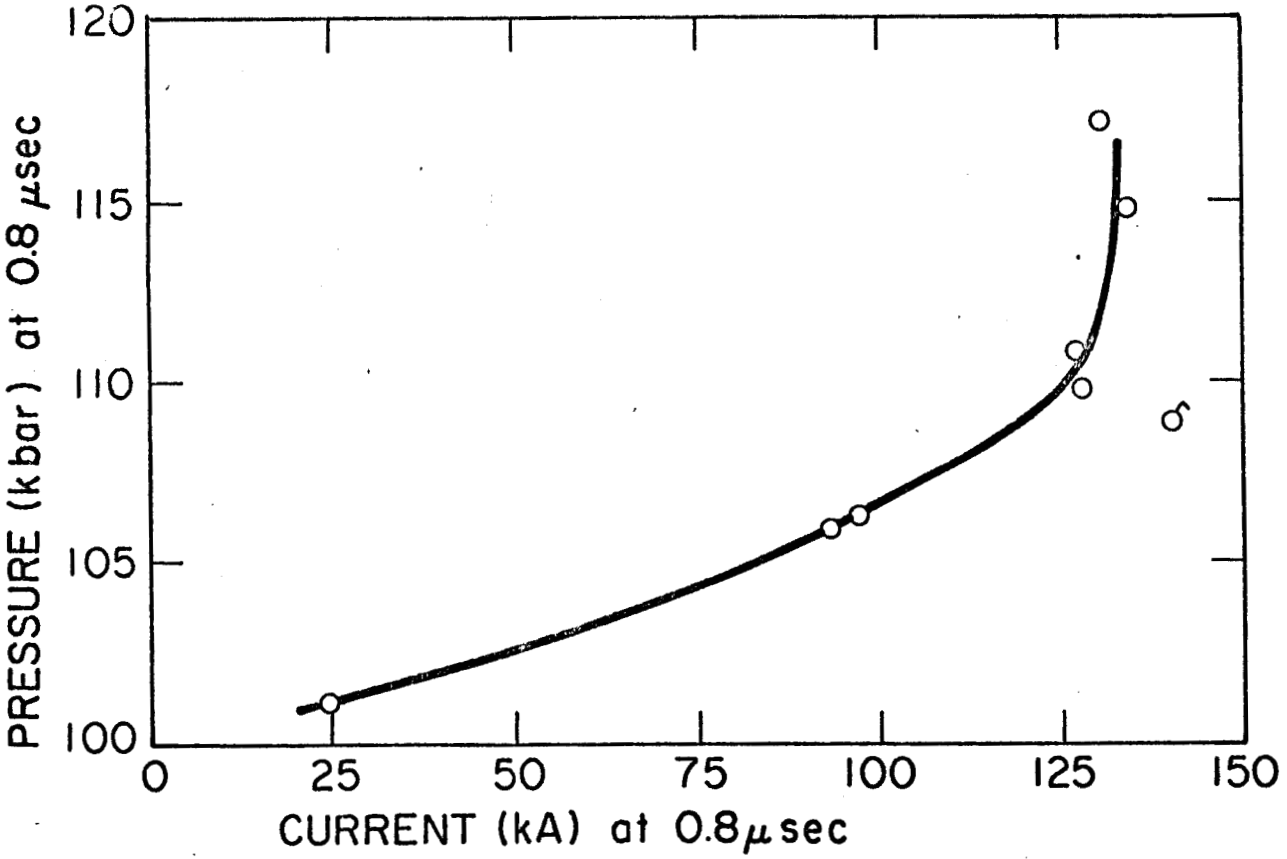


Fig. 8 James W. Robinson Jr. Appl. Phys.

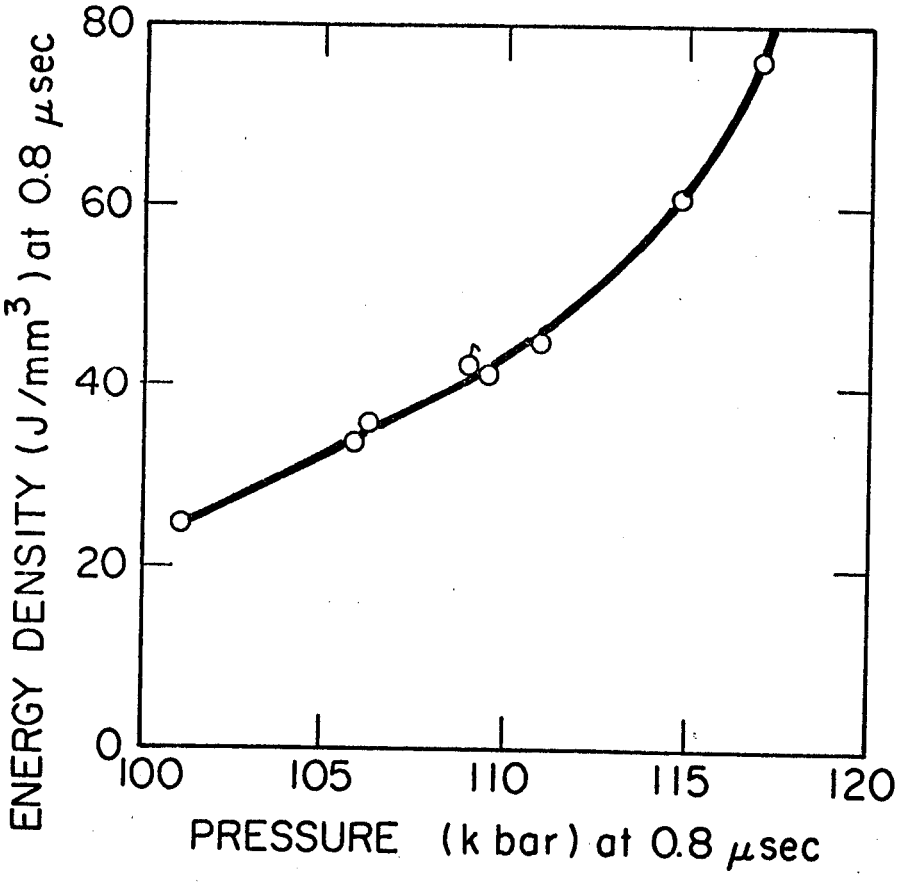


Fig. 9 James W. Robinson J Appl. Phys.

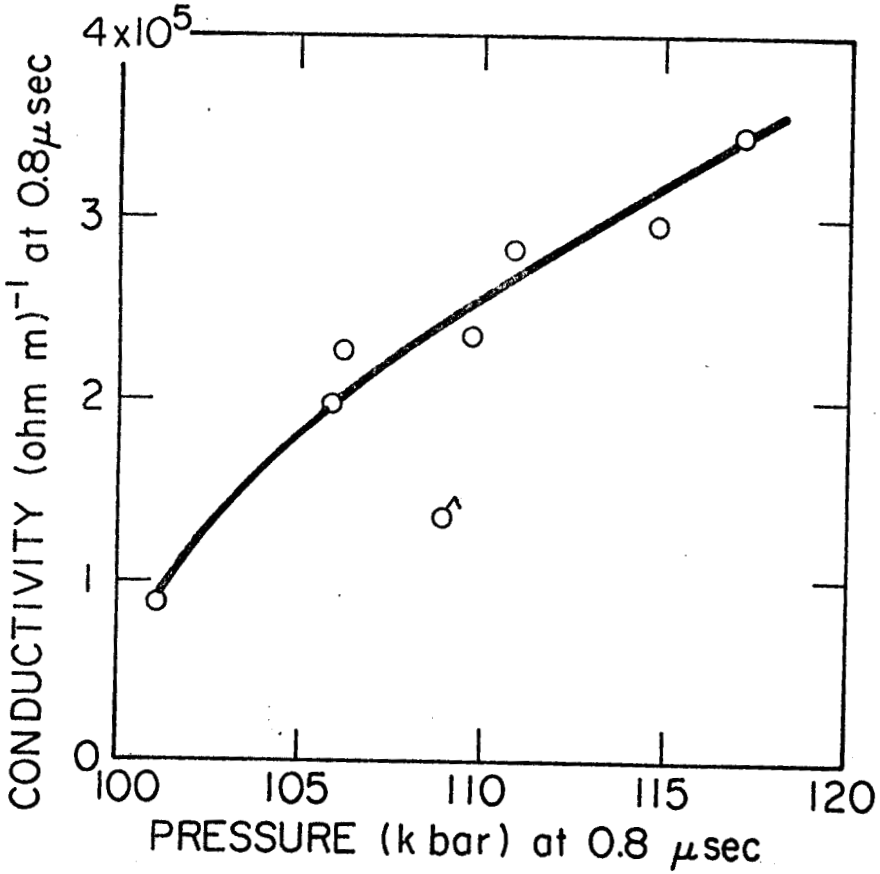


Fig 10 James W. Robinson J. Appl. Phys.

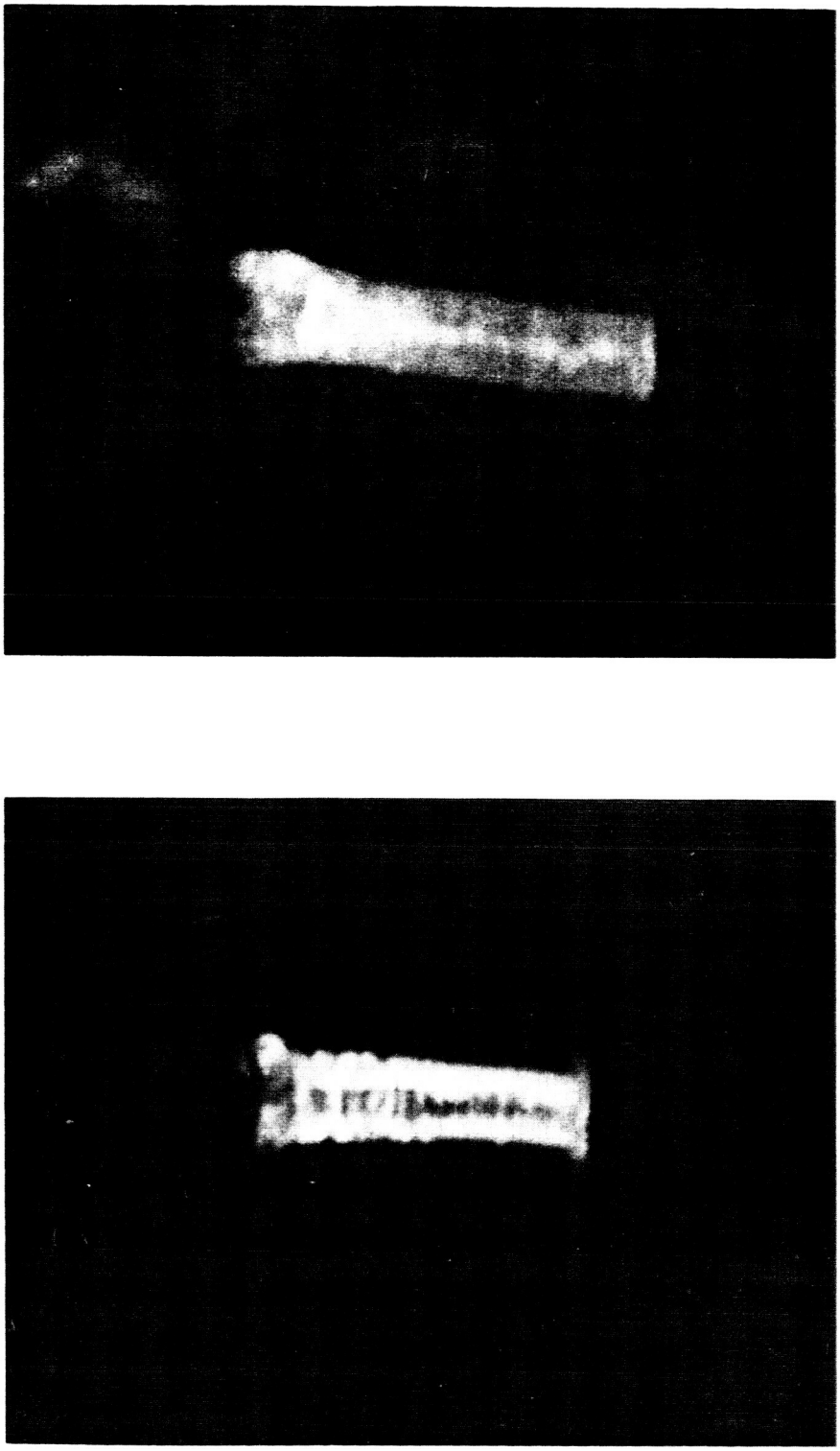

Fig. 11. Two photographs of plasma columns at 100 kilobars of pressure.

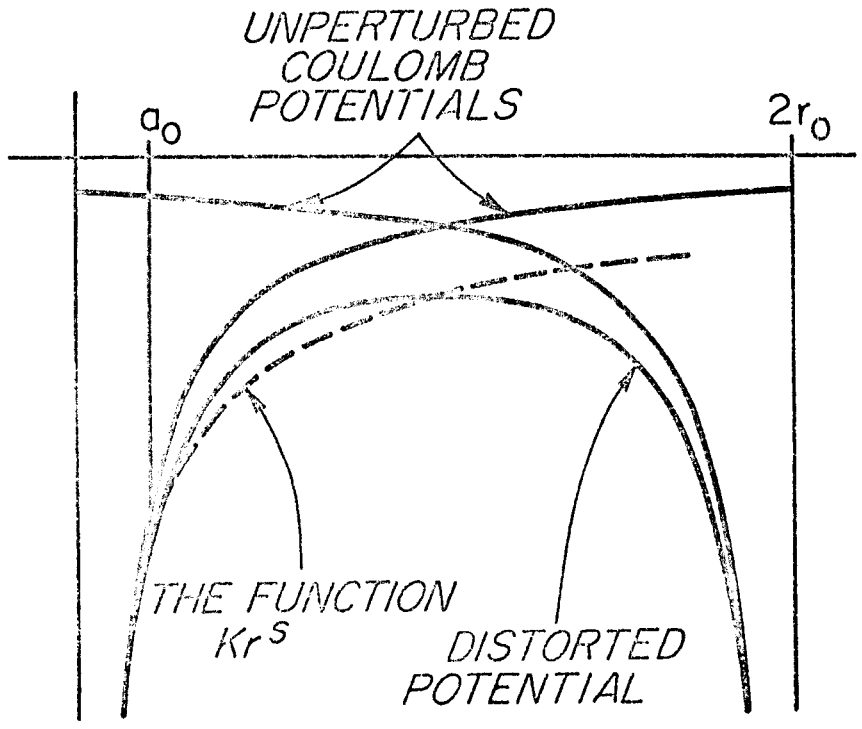


Fig 12, James W Robinson J. Appl. Phys.